EFFECT OF BROWNIAN DIFFUSION ON ELECTRICAL CLASSIFICATION OF ULTRAFINE AEROSOL PARTICLES IN DIFFERENTIAL MOBILITY ANALYZER

YASUO KOUSAKA, KIKUO OKUYAMA, MOTOAKI ADACHI AND TADAAKI MIMURA

Department of Chemical Engineering, University of Osaka Prefecture, Sakai 591

Key Words: Aerosol, Brownian Diffusion, Differential Mobility Analyzer, Electrical Classification, Particle Loss, Ultrafine Aerosol Particle

Effect of Brownian diffusion on the electrical classification of ultrafine particles in the differential mobility analyzer (DMA) has been studied theoretically and experimentally. Two kinds of particle losses which are undesirable in size analysis, (1) loss caused by the Brownian diffusion of particles traversing the sheath air stream toward the collector rod of the DMA, and (2) loss caused by Brownian diffusive deposition of particles on every wall of the DMA excluding the collector surface, were theoretically evaluated by solving the diffusion equation. Some of the calculation results were confirmed by experiments for particles of various sizes, two different lengths of DMA and various ratios of flow rate of aerosol to sheath air.

Introduction

The differential mobility analyzer (DMA) has been increasingly utilized as a sizing instrument as well as a monodisperse aerosol generator of particles smaller than 1 μm in diameter. In sizing of ultrafine particles of diameter less than 0.1 μm, however, the following two kinds of particle losses may be expected in the DMA: (1) loss caused by the Brownian diffusion of particles traversing the sheath air stream toward the collector rod, and (2) loss caused by the Brownian diffusive deposition of particles on every wall of the analyzer. These losses were evaluated theoretically by solving the diffusion equation and were experimentally observed in the tandem DMA system.

1. Theoretical Considerations

1.1 Electrical classification of particles in DMA

Figure 1(a) shows a schematic diagram of the DMA used in this study. It has almost the same dimensions as that reported by Knutson and Whitby[1] and that commercialized by TSI Co., Ltd. (TSI Model 3071). A polydisperse aerosol of unknown size is fed into the DMA. The collector-rod voltage and the flow rate are set at certain values such that aerosol particles of specific size range are drawn out from the DMA. When the Brownian motion of particles is negligible in the DMA, the center value of electrical mobility distribution Z_{pc} and half the mobility band ΔZ_p of the DMA outlet aerosol are given by the following equations:[1]

$$Z_{pc}(V)=[\{q_c+0.5(q_a-q_s)\}/2\pi L^B V]\ln(R/kR) \quad (1)$$

$$\Delta Z_p=\{(q_a+q_s)/4\pi L^B V\}\ln(R/kR) \quad (2)$$

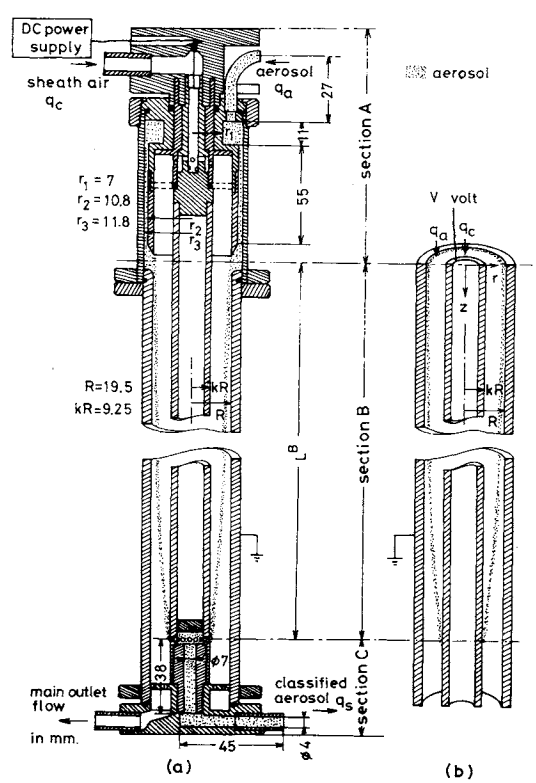

Fig. 1. Differential mobility analyzer.

Received February 21, 1986. Correspondence concerning this article should be addressed to Y. Kousaka. M. Adachi is at the Radiation Center of Osaka Prefecture, Sakai 593.

where q_c, q_a and q_s are the flow rates of sheath air, inlet aerosol and exit aerosol, respectively. It is expected, however, that Brownian diffusion cannot be neglected when the particle size is small. Particle losses caused by Brownian diffusion will take place in the following three sections: (1) inlet pipe and annular section before aerosol merges with sheath air (section A shown in Fig. 1 (a)); (2) electrical classification section (section B); and (3) section after sampling port (section C).

Changes in number concentration of aerosol particles in sections A, B and C can be evaluated by applying the diffusion equation as follows.

1) Brownian diffusion in electrical classification section (section B) Since the flow pattern of gas and aerosol in section B in the DMA is very difficult to analyze, this section is approximated to the system where aerosol and sheath air flow coaxially through the annular tube as shown in Fig. 1 (b). As reported in the previous paper,[3] the trajectory of a monodisperse particle undergoing Brownian motion is governed by the equation of convective diffusion, which is expressed as follows:

$$u(r)\frac{\partial n_p(r,z)}{\partial r}=D\left\{\frac{\partial^2 n_p(r,z)}{\partial r^2}+\frac{1}{r}\frac{\partial n_p(r,z)}{\partial r}+\frac{\partial^2 n_p(r,z)}{\partial z^2}\right\}-\frac{1}{r}\frac{\partial}{\partial r}\{Z_p r E(r) n_p(r,z)\} \tag{3}$$

where r and z denote the radial and axial coordinates, respectively, as shown in Fig. 1 (b), n_p the number concentration of particles carrying p elementary charges, $u(r)$ the axial velocity, D the Brownian diffusion coefficient, Z_p the electrical mobility of the particle and $E(r)$ the intensity of the electric field as given by the next equation.[1]

$$E(r)=V/\{r\ln(R/kR)\} \tag{4}$$

The following assumptions are made in the derivation of Eq. (3):

(1) Parabolic laminar flow is fully developed at the merging point of aerosol with sheath air ($z=0$).

(2) The inlet aerosol contains spherical and monodisperse particles with single elementary charge.

(3) The effect of Brownian coagulation and electrostatic diffusion on the change in particle number concentration can be ignored.

(4) There is no flow to the sampling ports ($q_s=0$).

The velocity profile of air in an annular tube is given as

$$u(r)=2u_{av}[1-(r/R)^2+\{(k^2-1)/\ln k\}\ln(r/R)]/\{(1-k^4)/(1-k^2)-(k^2-1)/\ln k\} \tag{5}$$

where $u_{av}=(q_a+q_c)/\pi(R^2-k^2R^2)$. When the value of the Peclet number ($=2Ru_{av}/D$) is larger than 100, Brownian diffusion in the axial direction can be ignored. Since this condition is valid for particles larger than 1 nm in diameter, the nondimensional expression of Eq. (3) is given as follows:

$$\frac{\partial \bar{n}_p(\bar{r},\bar{z})}{\partial \bar{z}}=\frac{\bar{D}}{\bar{u}(\bar{r})}\left\{\frac{\partial^2 \bar{n}_p(\bar{r},\bar{z})}{\partial \bar{r}^2}+\frac{1}{\bar{r}}\frac{\partial \bar{n}_p(\bar{r},\bar{z})}{\partial \bar{r}}\right\}+\frac{\bar{E}}{\bar{u}(\bar{r})\bar{r}}\frac{\partial \bar{n}_p(\bar{r},\bar{z})}{\partial \bar{r}} \tag{6}$$

where $\bar{r}=r/R$, $\bar{z}=z/L^B$, $\bar{n}_p(\bar{r},\bar{z})=n_p(r,z)/n_{in}^B$, $\bar{u}(\bar{r})=u(r)/u_{av}$. $\bar{D}$ and $\bar{E}$ in Eq. (6) are the dimensionless parameters which can be evaluated from the aerosol property and the dimensions of the mobility analyzer as follows.

$$\bar{D}=DL^B/R^2u_{av} \quad \text{and} \quad \bar{E}=Z_pL^BV/R^2u_{av}\ln k \,. \tag{7}$$

The initial and boundary conditions for Eq. (6) are:

$$\bar{n}_p(k,\bar{z})=0 \quad \text{and} \quad \bar{n}_p(1,\bar{z})=0 \qquad \text{at} \quad \bar{z}\geq 0$$
$$\bar{n}_p(\bar{r},0)=0 \qquad \text{at} \quad k\leq\bar{r}<\delta$$
$$\bar{n}_p(\bar{r},0)=1 \qquad \text{at} \quad \delta\leq\bar{r}<1$$

where δ shows the ratio of the thickness of the clean air stream to the whole gas stream and can be obtained from the following relation.

$$q_a=2\pi u_{av}R^2\int_\delta^1 \bar{u}(\bar{r})\bar{r}d\bar{r} \tag{8}$$

Since Eq. (6) cannot be solved analytically, the Crank-Nicolson implicit method was employed to solve it. The diffusion equation, Eq. (6), is converted to finite difference equations using a simple central difference formula. The solution requires the numerical calculation of a set of algebraic equations whose matrix is tridiagonal and is easily completed by a Gaussian elimination process.

Numerical calculations were made with various mesh points to check their accuracy, and a mesh of 1000 radial points and 1000 axial points was found to be sufficient. The average number concentration of aerosol particles in an axial plane at any arbitrary distance z can be given from the numerical solution of Eq. (6) as follows.

$$\bar{n}_{av}(\bar{z})=2\pi\int_k^1 \bar{n}_p(\bar{r},\bar{z})\bar{u}(\bar{r})\bar{r}d\bar{r}\Big/2\pi\int_k^1 \bar{u}(\bar{r})\bar{r}d\bar{r} \tag{9}$$

Figure 2 shows the decrease in average particle number concentration of monodisperse particles having one elementary charge, where the ordinate indicates the average particle number concentration remaining in the DMA and the abscissa is the dimensionless length. In this figure, V_c is the applied voltage required to bring a singly charged particle to the sampling port of the DMA ($V_c=q_c\ln(R/kR)/2\pi L^BZ_p$). The thin straight solid line shows the calculated result of no Brownian diffusion and other lines

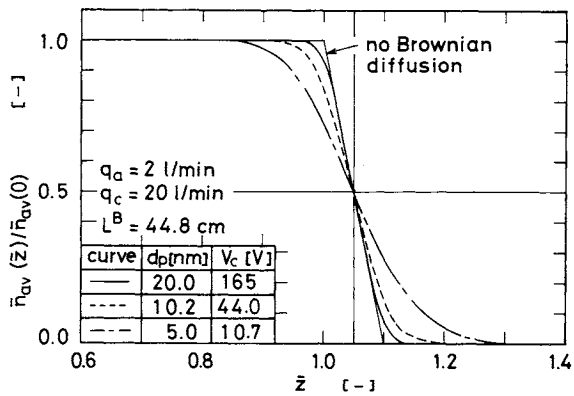

Fig. 2. Change of average particle number concentration in electrical classification process.

show results when Brownian diffusion takes place.

Figure 3 shows the deposition flux of particles toward the inner cylinder, calculated by the next equation.

$$j = -D\partial n_p/\partial r\big|_{r=kR} + Z_p V n_p/(r \ln k)\big|_{r=kR} \quad (10)$$

In the case of no Brownian diffusion, all particles reaching between 1 and $1+\Delta\bar{z}$, where $\Delta\bar{z}$ is expressed by $\Delta\bar{z}=q_a/q_c$, will be sucked through the sampling port. Since the region where particles deposit on the collector rod is spread due to Brownian diffusion as seen in Fig. 3, only particles reaching the center rod between 1 and $1+\Delta\bar{z}$ are sucked through if there is gas flow through the sampling ports, and particles reaching the region outside the $\Delta\bar{z}$ cannot be sampled. This loss of particles may be called sampling efficiency and is expressed by the following equation:

$$S^B(V) = N^B_{out}/N^B_{in} \quad (11)$$

where N^B_{in} and N^B_{out} are the particle numbers of fed and sampled aerosol per unit time, respectively, and are expressed by the following equations:

$$N^B_{in} = q_a n_p(r, 0) \qquad \text{at} \quad \delta \le r < R \quad (12)$$

$$N^B_{out} = \int_{L^B}^{L^B(1+\Delta\bar{z})} 2\pi k R j(V, z) dz \quad (13)$$

The distribution of the deposited particles (deposition flux j) changes according to the applied voltage V as shown in **Fig. 4**. When V is higher or lower than V_c, only particles deposited in the range from 1 to $1+\Delta\bar{z}$ are sampled, as indicated by shadow lines in Fig. 4. When V equals V_c, the center of the flux distribution coincides with the center of sampling zone, $\bar{z}=1+\Delta\bar{z}/2$, and the sampling efficiency is highest. Changes in the ratio of sampled particles to the total, that is, sampling efficiency, are shown in **Fig. 5**. Since the relative importance of Brownian diffusion to electrical classification can be evaluated by the dimensionless parameter $\bar{D}/\bar{E}=D\ln(1/k)/Z_pV$, the sampling

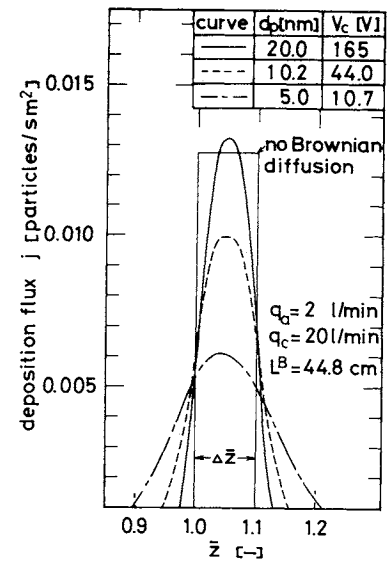

Fig. 3. Deposition flux of particle toward inner cylinder.

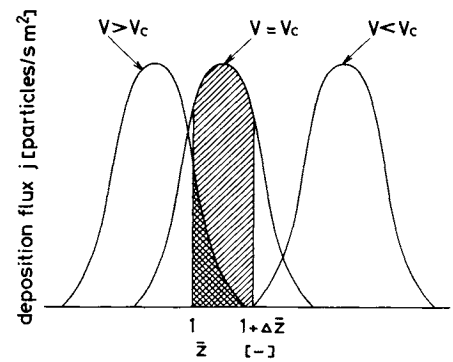

Fig. 4. Illustration of change in distribution of deposition flux with applied voltage.

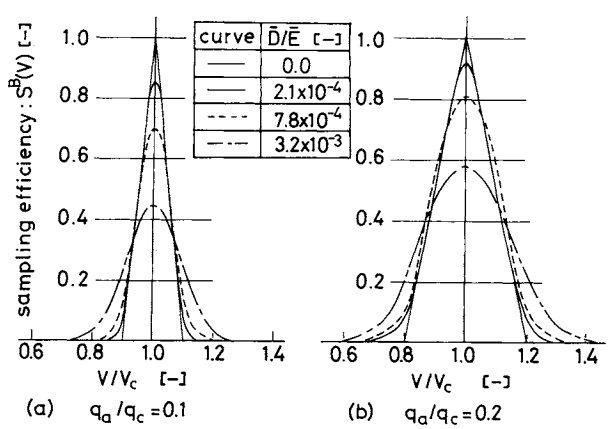

Fig. 5. Effect of Brownian diffusion on sampling efficiency.

efficiency $S^B(Z_p)$ can be expressed as a function of $\bar{D}/\bar{E}$. The thin straight solid line is the sampling efficiency of no Brownian diffusion. It is seen that the sampling efficiency curves are broadened by Brownian diffusion with decreasing particle size.

The abscissa of this figure can be replaced by the ratio of electrical mobility $Z_{pc}(V)/Z_{pc}(V_c)$ by introducing Eq. (1). Therefore, the sampling efficiency

for the electrical mobility Z_p, $S^B(Z_p)$ has quite the same distribution as shown in Fig. 5.

Figure 6 shows the effect of $\bar{D}/\bar{E}$ on the sampling efficiency calculated. The ordinate is the sampling efficiency $S^B(Z_p)_{V=V_c}$ when the applied voltage V equals to V_c. It is found from Fig. 6 that the sampling efficiency of $q_a/q_c=0.2$ is higher than that of $q_a/q_c=0.1$ and is approximately unity when $\bar{D}/\bar{E}$ is less than 10^{-5}, that is, the effect of Brownian diffusion is almost ignored.

2) Brownian diffusion in other parts (sections A and C) Since there exists no electric field in sections A and C as shown in Fig. 1 (a), the decrease in particle number concentration is mainly caused by Brownian diffusion, which is given by the numerical solution of Eq. (6) without electric field. Details of sections A and C are shown in Fig. 1 (a).

Figure 7 shows the penetration of aerosol particles in sections A and C, which is numerically calculated. Particle loss in section A is larger than that in section C.

1.2 Electrical classification of particles in tandem DMAs

Now, we discuss the tandem DMA system, where the exit aerosol from the first DMA is directly admitted into the second DMA without passing through a neutralizer, and the flow rates of aerosol and sheath air of the second DMA are set equal to those of the first DMA. This system is useful for measuring particle growth or evaporation[4] and to calibrate DMAs.

The electrical mobility distribution function of the first DMA exit aerosol, n_{1o}, can be expressed as the product of its function at inlet, $n_{1i}(Z_p)$, and the sampling efficiency $S(Z_p)$:

$$n_{1o}(Z_p)=n_{1i}(Z_p)S_1^A(Z_p)S_1^B(Z_p)S_1^C(Z_p) \qquad (14)$$

where

$$S_1^A(Z_p)=n_{out}^A/n_{in}^A$$

$$S_1^C(Z_p)=n_{out}^C/n_{in}^C$$

The number concentration of the exit aerosol Δn_{1o} at a certain collector-rod voltage is given as:

$$\Delta n_{1o}=\int_{Z_{p1}}^{Z_{p2}} n_{1o}(Z_p)dZ_p \qquad (15)$$

where Z_{p1} and Z_{p2} are the smallest and largest electrical mobilities of the first DMA exit aerosol, respectively. When the collector-rod voltage of the second DMA V_2 is varied while that of the first DMA V_1 is maintained constant, the second DMA exit aerosol concentration-voltage response curve can be obtained. In **Fig. 8**, the solid curve shows the electrical mobility distribution of aerosol classified in the first DMA and supplied into the second DMA. When the collector-rod voltage at the second DMA is fixed at a

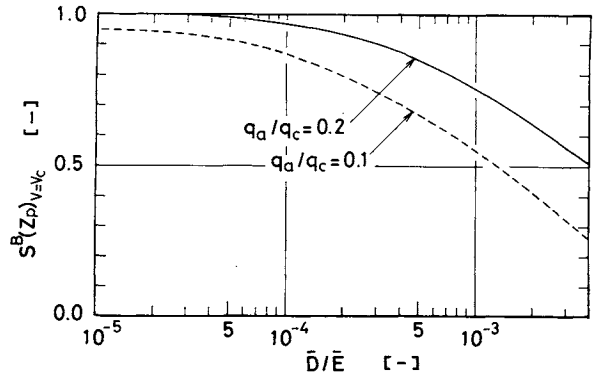

Fig. 6. Change in sampling efficiency with dimensionless parameter $\bar{D}/\bar{E}$.

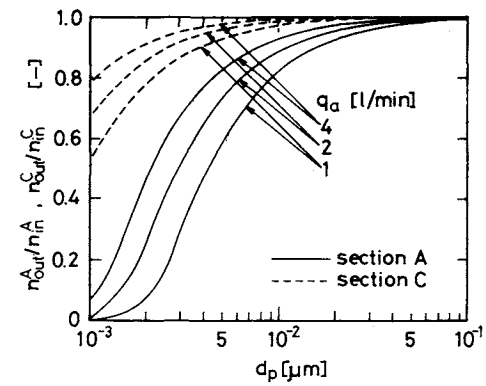

Fig. 7. Penetration of monodisperse particles in sections A and C.

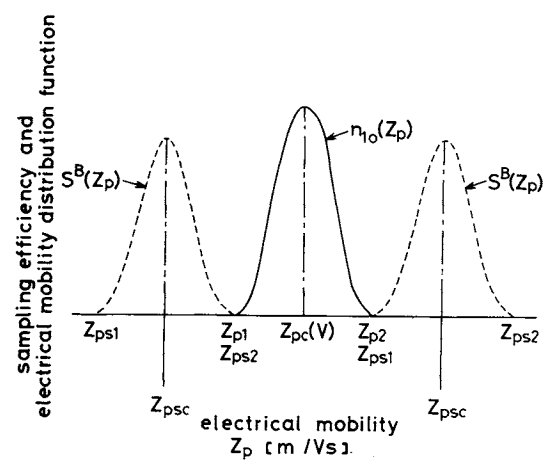

Fig. 8. Illustration of sampling efficiency $S^B(Z_p)$ and electrical mobility distribution function $n_{1o}(Z_p)$.

certain value, the center value of electrical mobility Z_{psc} which gives the maximum sampling efficiency is determined. In this figure, Z_{ps1} and Z_{ps2} indicate the electrical mobilities which give minimum sampling efficiency. If the setting of the voltage of the second DMA is smaller than that corresponding to $Z_{p2}+\{Z_{p2}-Z_{pc}(V)\}$ or larger than $Z_{p1}-\{Z_{pc}(V)-Z_{p1}\}$, the particle number concentration of the second DMA exit will be zero, as shown in Fig. 8, whereas it is not zero if the voltage is set at a value between

these two limits.

The general equation that gives the Z_p distribution function of the second DMA exit aerosol, $n_{2o}(Z_p)$, can be expressed as follows:

$$n_{2o}(Z_p)=n_{1o}(Z_p)S_2^A(Z_p)S_2^B(Z_p)S_2^C(Z_p) \qquad (16)$$

The number concentration of the second DMA exit aerosol, Δn_{2o}, at a certain collector-rod voltage, is given as:

$$\Delta n_{2o}=\int_{Z_{p1}}^{Z_{p2}} n_{2o}(Z_p)dZ_p \qquad (17)$$

The change in particle number concentration of the second DMA exit with the second collector-rod voltage V_2 can be calculated from Eq. (17), and the result is shown in **Fig. 9**. When the effect of particle losses by Brownian diffusion is negligible, the value of $\Delta n_{2o}/\Delta n_{1o}$ is 0.667 at $V_2/V_1=1.0$ as discussed in the previous paper.[3] However, it is found from Fig. 9 that the effect of Brownian diffusion becomes significant with decreasing particle size, as indicated by broader and lower voltage-number concentration response curves.

2. Experimental Considerations

2.1 Experimental apparatus and method

Figure 10 shows a schematic diagram of the apparatus used in the experiment. A polydisperse NaCl aerosol of particle diameter from 4 to 60 nm was produced by an evaporation-condensation aerosol generator.[2] The aerosol was passed through the Am-241 (100 μCi) neutralizer and was fed into the first DMA. The sheath air was recirculated; this means $q_s=q_a$. The classified aerosol exiting from the first DMA was directly fed into the second DMA, without passing through the neutralizer. The particle number concentrations of aerosol at the inlet and the exit of the second DMA were measured by the condensation nucleus counter (CNC).[2,4]

In this experiment, three different DMAs were used as the second DMA, as shown in **Table 1**. DMAs I and II have shorter length of section B than DMA III so as to learn the effect of Brownian diffusion, and the material of section C of DMA I is brass rather than Teflon, as shown in **Fig. 11**, so as to learn the effect of electrostatic deposition. They were operated under the same conditions as the first DMA.

2.2 Experimental results and discussion

Figure 12 shows the ratio of the particle number concentration of the second DMA exit aerosol to that of the first DMA exit aerosol when a collector-rod voltage corresponding to $Z_{psc}=Z_{pc}$ is applied to the first and second DMA. The keys of solid circle, open circle and triangle indicate the experimental results for DMAs I, II and III, respectively. The solid and one-point dashed curves are the calculation results

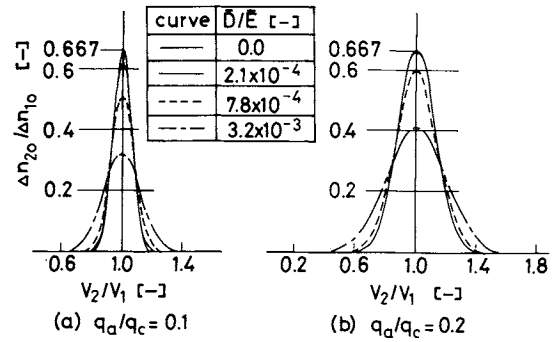

Fig. 9. Particle number concentration of second DMA exit aerosol.

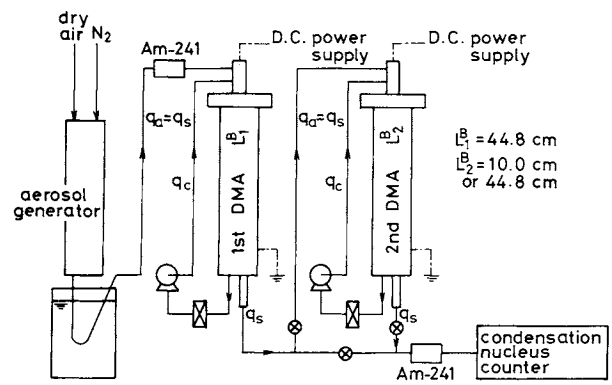

Fig. 10. Schematic diagram of experimental apparatus.

Table 1. Dimensions and material of second DMA

DMA	Length of section B (L_2^B)	Material of section C in Fig. 11
I	10.0 cm	Brass (type B)
II	10.0 cm	Teflon (type A)
III	44.8 cm	Teflon (type A)

1) DMA III is quite the same in dimensions as for the first DMA.
2) Other dimensions except L_2^B of DMAs I and II are quite the same as for the first DMA.

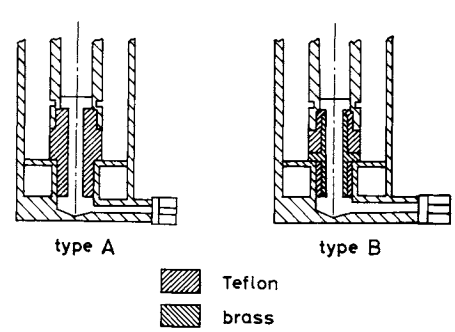

Fig. 11. Details of section C.

obtained by Eq. (17) considering Brownian diffusion in the length of section B of $L_2^B=10$ cm and 44.8 cm, respectively. The dotted lines are the theoretical results under no effect of Brownian diffusion. From both results for aerosol flow rates q_a of 2 l/min and

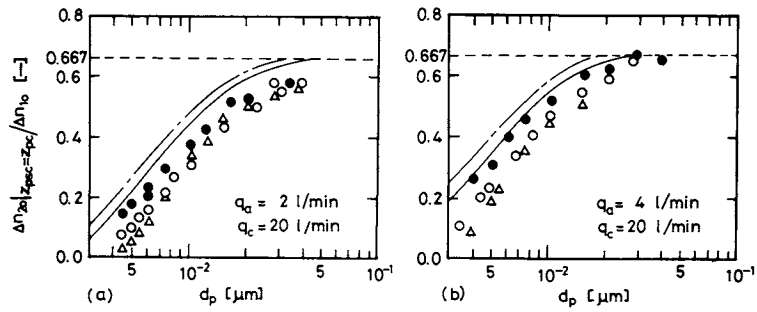

experimental results				calculated results	
DMA	key	L_2^B [cm]	material	curve	L_2^B [cm]
I	●	10	brass	- - -	10
II	○	10	Teflon	——	44.8
III	△	44.8	Teflon		

Fig. 12. Response of second DMA exit concentration when collector-rod voltage corresponding to $Z_{psc}=Z_{pc}$ is applied to first and second DMA.

4 l/min it is found that the particle deposition in section C made of Teflon is enhanced compared with that made of brass due to the electrostatic force which may be induced by the charge on Teflon walls. The comparison of DMA II ($L_2^B=10$ cm) and DMA III ($L_2^B=44.8$ cm) shows the slight effect of Brownian diffusion in section B on particle number concentration of exit aerosol. On the other hand, the experimental results for $q_a=4$ l/min show higher concentration and agree better with the theoretical results than that for $q_a=2$ l/min. Furthermore, no loss of particle appears in the range of size larger than about 20 nm in diameter. This reason may be (i) particle loss by a slight disturbance at the point where aerosol merges with sheath air and (ii) rough approximation of aerosol paths in sections A and C.

Figure 13 shows the particle number concentrations sampled from the second DMA together with the corresponding calculation results obtained by Eq. (17). The collector-rod voltage of the first DMA, V_1', is kept constant, while the second DMA voltage V_2 is varied. The ordinate is the ratio of number concentration of the second DMA exit aerosol to that of the second DMA inlet, $\Delta n_{2o}/\Delta n_{1o}$. The abscissa is the ratio of the second DMA collector-rod voltage to the first one, V_2/V_1, where V_1 is $V_1'L_2^B/L_1^B$. Figure 13(a) shows the experimental results using DMA III as the second DMA. In both cases of $q_a=2$ l/min and 4 l/min, the experimental results have peaks at $V_2/V_1=1$ and their distributions tend to broaden with decreasing particle size as the theoretical curves show. It is found from this figure that no particle loss caused by Brownian diffusion appears in the size range of larger than 20 nm and at the operating conditions of $q_a=4$ l/min and $q_c=20$ l/min. It is also seen that the experimental data in all cases deviated toward lower voltages of V_2. This nonsymmetry seen in the distribution is considered to be caused by the difference in Brownian diffusion coefficient due to particle size.

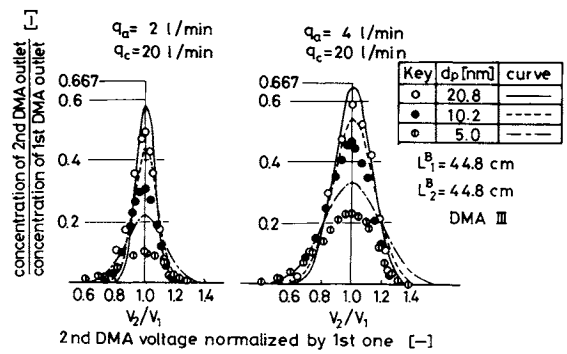

Fig. 13(a). Response of second DMA exit concentration when second DMA collector-rod voltage is changed.

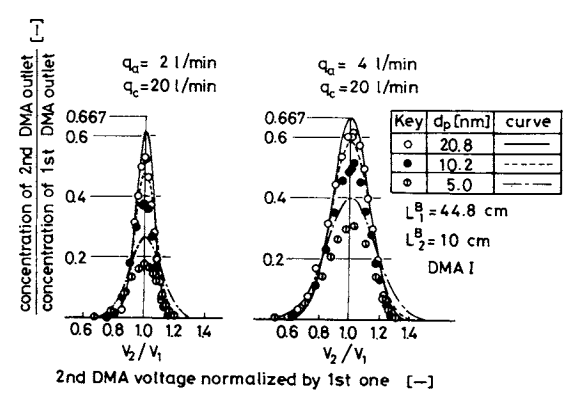

Fig. 13(b). Response of second DMA exit concentration when second DMA collector-rod voltage is changed.

Figure 13 (b) shows the results for DMA I, which has short length of section B, $L_2^B=10$ cm. The experimental results for this DMA show quite the same tendency as those for DMA III. The number concentrations of sampled particle with DMA I are higher than those with DMA III in the size range of smaller than 10 nm. This suggests that the shortening of length of section B and the change of material of section C are effective in increasing the concentration of sampled particles as far as small particles are concerned.

Conclusion

The effect of Brownian diffusion on the electrical classification of ultrafine aerosol particles in differential mobility analyzers was studied theoretically and experimentally. The results obtained in this work are as follows.

1. The particle loss due to Brownian diffusion of particles traversing the sheath air stream toward the collector rod increased with decreasing particle size and flow rate of clean sheath air. The particle loss becomes significant when the dimensionless parameter $\bar{D}/\bar{E}$ is larger than 10^{-5}.

2. Due to Brownian diffusion, the electrical mobility distribution of classified aerosol becomes broader and lower compared with that obtained under no effect of Brownian diffusion.

3. Some of the calculation results almost agreed with the experimental results for particles of various sizes, and various collector rod lengths of DMAs and flow ratios of aerosol to sheath air.

Acknowledgment

The authors are greatly indebted to Dr. G. M. Sem in TSI Co., Ltd., for the kind offer of a DMA having shorter length than commercial ones, and also to Dr. A. Mizohata in the Radiation Center of Osaka Prefecture for the use of a computer (ACOS-4) in this study.

Nomenclature

D = diffusion coefficient of a particle [$m^2 s^{-1}$]
$\bar{D}$ = dimensionless parameter ($=DL^B/R^2u_{av}$) [—]
d_p = particle diameter [m]
$E(r)$ = strength of electric field [$V m^{-1}$]
$\bar{E}$ = dimensionless parameter ($=Z_p(V)L^BV/R^2u_{av}\ln k$) [—]
$j(V, z)$ = deposition flux [$m^{-2} s^{-1}$]
k = ratio of outer radius of center-rod to inner radius of mobility analyzer housing [—]
L^B = length of section B of DMA [m]
N^B_{in}, N^B_{out} = particle number per unit time at inlet and exit of electrical classification section, respectively [s^{-1}]
$\bar{n}_{av}(\bar{z})$ = dimensionless average number concentration of particles [—]
n_{in}, n_{out} = average particle number concentration at inlet and exit of each section of DMA [m^{-3}]
$n_p(r, z)$ = number concentration of particle carrying p elementary charge [m^{-3}]
$\bar{n}_p(\bar{r}, \bar{z})$ = dimensionless number concentration of particle carrying p elementary charge [—]
$n_{1i}(Z_p), n_{1o}(Z_p)$ = mobility distribution function of fed and exit aerosol of first DMA [$Vs m^{-5}$]
$n_{2o}(Z_p)$ = mobility distribution function of exit aerosol of second DMA [$Vs m^{-5}$]
q_a, q_c, q_m, q_s = flow rates of fed aerosol, sheath air, main exit flow and exit aerosol, respectively [$m^3 s^{-1}$]
R = inner radius of mobility analyzer housing [m]
r = radial coordinate [m]
$\bar{r}$ = dimensionless radial coordinate ($=r/R$) [—]
$S(V)$ = sampling efficiency for applied voltage [—]
$S(Z_p)$ = sampling efficiency for particle having electrical mobility Z_p [—]
$u(r)$ = axial velocity of air [$m s^{-1}$]
$\bar{u}(\bar{r})$ = dimensionless axial velocity of air [—]
u_{av} = mean velocity of air [$m s^{-1}$]
V = center-rod voltage of DMA [V]
V_c = center-rod voltage needed to bring a certain particle to center of sampling port [V]
Z_p = electrical mobility of particle [$m^2 V^{-1} s^{-1}$]
$Z_{pc}(V)$ = center value of electrical mobility band [$m^2 V^{-1} s^{-1}$]
Z_{p1}, Z_{p2} = minimum and maximum electrical mobilities, respectively, of classified aerosol [$m^2 V^{-1} s^{-1}$]
Z_{psc} = electrical mobility which gives maximum sampling efficiency [$m^2 V^{-1} s^{-1}$]
Z_{ps1}, Z_{ps2} = electrical mobilities which give minimum sampling efficiency as shown in Fig. 8 [$m^2 V^{-1} s^{-1}$]
z = axial coordinate [m]
$\bar{z}$ = dimensionless axial coordinate ($=z/L^B$) [—]

$\Delta n_{1o}, \Delta n_{2o}$ = particle number concentration of exit aerosol of first and second DMAs, respectively [m^{-3}]
$\Delta\bar{z}$ = dimensionless distance of sampling region ($=q_a/q_c$) [—]
ΔZ_p = half value of electrical mobility band [$m^2 V^{-1} s^{-1}$]
δ = width of aerosol flow at inlet of electrical classification process [m]

〈Superscripts〉
A, B, C = of sections A, B and C in DMA, respectively

〈Subscripts〉
1, 2 = of the first and second DMAs, respectively

Literature Cited

1) Knutson, E. O. and K. T. Whitby: *J. Aerosol Sci.*, **6**, 443 (1975).
2) Kousaka, Y., T. Niida, K. Okuyama and H. Tanaka: *J. Aerosol Sci.*, **13**, 231 (1982).
3) Kousaka, Y., K. Okuyama and M. Adachi: *Aerosol Sci. Technol.*, **4**, 209 (1985).
4) Kousaka, Y., K. Okuyama, T. Niida, T. Mimura and T. Hosokawa: *Part. Charact.*, **2**, 119 (1985).